Title:

In-situ Microwave-assisted Catalytic Upgrading of Heavy Oil: Experimental Validation and Effect of Catalyst Pore Structure on Activity

Author names and affiliations:

Mohamed Adam [a], Hossein Anbari [a], Abarasi Hart [b], Joseph Wood [b], John P. Robinson [a] and Sean P. Rigby [a]

[a] Faculty of Engineering, University of Nottingham, Nottingham NG7 2RD, UK

[b] School of Chemical Engineering, University of Birmingham, Birmingham B15 2TT, UK

Author e-mail addresses:

Mohamed Adam: mohamed.adam@nottingham.ac.uk

Hossein Anbari: hossein.anbari@nottingham.ac.uk

Abarasi Hart: hartabarasi@yahoo.com

Joseph Wood: j.wood@bham.ac.uk

John P. Robinson: john.robinson@nottingham.ac.uk

Sean P. Rigby: sean.rigby@nottingham.ac.uk

Corresponding authors:

Mohamed Adam: mohamed.adam@nottingham.ac.uk

Sean P. Rigby: sean.rigby@nottingham.ac.uk

Abstract

In-situ combustion alone may not provide sufficient heating for downhole, catalytic upgrading of heavy oil in the Toe-to-Heel Air Injection (THAI) process. In this study, a new microwave heating technique has been proposed as a strategy to provide the requisite heating. Microwave technology is alone able to provide rapid heating which can be targeted at the catalyst packing and/or the incoming oil in its immediate vicinity. It was demonstrated, contrary to previous assertions, that heavy oil can be heated directly with microwaves to 425°C, which is the temperature needed for successful catalytic upgrading, without the need for an additional microwave susceptor. Upgrading of > 3.2° API points, a reduction in viscosity to less than 100 cP, and > 12% reduction in sulfur content was achieved using commercially available hydrodesulfurization (HDS) catalyst. The HDS catalyst induced dehydrogenation, with nearly 20% hydrogen detected in the gas product. Hence, in THAI field settings, part of the oil-in-place could be sacrificed for dehydrogenation, with the produced hydrogen directed to aid hydrodesulfurization and improve upgrading. Further, this could provide a route for downhole hydrogen production, which can contribute to the efforts towards the hydrogen economy. A single, unified model of evolving catalyst structure was developed. The model incorporated the unusual gas sorption data, computerized x-ray tomography and electron microprobe characterization, as well as the reaction behavior. The proposed model also highlighted the significant impact of the particular catalyst fabrication process on the catalytic activity.

Keywords: microwave heating, in-situ catalytic upgrading, heterogeneous catalysis, heavy oil, catalyst characterization.

1 Introduction

Despite the encouraging growth in sustainable energy sources, oil and gas are still expected to satisfy up to 50%* of the world's energy demand in 2050 [1]. Hence, they will continue to act as the primary provider of energy security, contributing towards future growth while the necessary investment and technology development takes place in the transition towards renewable fuels. Further, parallel development in tools for mitigating the environmental impact of burning carbon-based fuels is also needed. Indeed, promising progress has already been made in CO_2 capture, utilization and storage (CCUS) technologies [2]. In addition to their energy uses, oil and gas are considered the primary feedstock to around 90% of chemicals produced around the world, and it is projected that petrochemicals will become the largest driver for global oil consumption by 2050 [3]. More recently, attempts have been made to develop techniques for in-situ production and extraction of hydrogen from oil reservoirs, leaving the carbon and other pollutants in the ground [4].

With the decline in light oil reserves attention has been shifting towards unconventional oil, such as heavy oils and bitumen which account for around 70% of total oil reserves [5]. Heavy oils and bitumen are asphaltic, dense and viscous oils with viscosities ranging from 100 cP (0.1 Pa.s) to more than 10,000 cP (10 Pa.s), and an American Petroleum Institute (API) gravity of less than 22.3° [6]. They have little, or no, mobility under reservoir conditions, which makes it difficult for them to be extracted using the same methods as conventional oil. Much of the current production of heavy oils and bitumen is achieved through opencast mining methods. However, these methods have severe environmental implications in terms of air pollution and groundwater contamination, as well as their large infrastructure footprint and the removal of the overlying countryside. Over the last few decades a number of

* These projections were made before the recent global COVID-19 pandemic, which has disturbed the energy sector and affected oil prices.

advanced techniques have been developed to facilitate in-situ extraction and recovery of heavy oils and bitumen [7, 8]. Among them, Toe-to-Heel Air Injection (THAI) with its catalytic add-on (CAPRI, CAtalytic upgrading PRocess in-situ) is considered one of the most promising technologies for simultaneous recovery and in-situ upgrading of heavy oils due to considerably lower environmental footprint than other extraction methods.

THAI is an in-situ combustion (ISC) process, making use of horizontal drilling technologies, in which air is injected into the reservoir to burn a small fraction of the oil. The generated heat thermally-cracks and mobilizes the oil ahead of the combustion front, which then drains into a horizontal producer well [9]. The catalytic add-on, CAPRI, potentially provides in-situ upgrading by surrounding the horizontal producer with a catalyst packing.

The special feature of the THAI-CAPRI process is the ‘moving window’ effect, which is a very different manner of operation of a catalytic reactor compared to many conventional surface processes. This refers to the fact that the flame front, and the various zones ahead of it, including the mobile oil zone, only spend up to three days in proximity to each particular section of the catalyst bed along the horizontal well. The actual operation period of a given section of catalyst in THAI-CAPRI thus corresponds to what would normally be only considered the initial, and transient, induction period at start-up of conventional, surface processes. Hence, THAI-CAPRI is special in that what might be considered merely the transient induction stage elsewhere actually corresponds to the main period of utilised activity of the catalyst. Otherwise transient phenomena in conventional processes thus take on much more significance in THAI-CAPRI. Each successive section of catalyst is utilised in turn in transient start-up operation as the flame front and active zones transit the whole length of the horizontal well. Just as the eventual pseudo-steady-state operation of a conventional reactor is determined by what happens in the transient induction period, then the behaviour during that

transient induction period is determined by the very earliest period of catalyst utilisation. The transient operation of the catalyst also demonstrates the need for use of a very rapid heating process like microwaves.

Hydrodesulfurisation (HDS) catalysts such as CoMo/γ-Al_2O_3 and NiMo/γ-Al_2O_3, which are commonly used in oil refineries, have given positive results when used in CAPRI tests at lab-scale [10, 11]. Studies using such catalysts showed that a temperature of around 425°C is needed for successful catalytic upgrading [10]. However, complementary reservoir simulation studies of the THAI process alone suggested that the actual temperature of the oil passing through catalyst packing around the horizontal well does not exceed 300°C [12]. Hence, there is a need to provide extra heating of the field-scale CAPRI reactor.

Electromagnetic heating methods have recently been proposed as possible strategies to overcome this deficiency and provide the additional heating needed for a successful CAPRI process [13, 14]. Hart and co-workers [15] demonstrated, in lab-scale tests, that inductive heating can be used to provide the heating needed for the catalytic upgrading. However, neither the oil nor the HDS catalyst interacted with the applied magnetic field at levels that were high enough to generate the heat needed to raise and maintain the temperature at 425°C. These workers needed to mix the catalyst with steel balls to act as a susceptor, with a catalyst-to-steel-balls volume ratio of about 2:1.

In the current study, microwave heating is proposed as an alternative to provide the requisite additional heating and increase the temperature at the catalyst packing and/or the oil in its immediate vicinity to the required 425 °C or more, without needing addition of susceptors. Microwave heating is a selective and volumetric heating technique whereby the heating can be targeted where specifically needed in the THAI-CAPRI process. Unlike conventional conductive and convective heating methods heating is achieved instantaneously, as a result of

the interaction of the electromagnetic field with the material at the molecular and/or sub-molecular levels. The electromagnetic field can penetrate the rock matrix, allowing heating to take place at a significant distance away from the electromagnetic source. Therefore, in a THAI-CAPRI setting, heating can be targeted at the catalyst packing, and/or the incoming oil in its immediate vicinity, at any desired section along the horizontal well to correspond to any part of the combustion front and successive layers.

Where a number of studies have been published on microwave-assisted processing and upgrading of heavy oils, many of these studies have erroneously concluded that microwaves can only be used for heating the oil by indirect means, i.e. via the use of a microwave susceptor such as activated carbon [16], silicon carbide (SiC) [17] or carbon nanoparticles [18]. The need for microwave susceptors is supposedly because of the relatively low microwave-absorbing ability of the oils themselves, and also because of the lack of proper applicator/cavity design since most of the previous studies were conducted in modified domestic microwave ovens. Domestic ovens are built with limited power and low levels of electric field intensity, and they lack a well-defined electric field configuration.

However, we have recently [14] shown that at high temperatures, which is the case in THAI-CAPRI, heavy oils are themselves more susceptible to being heated directly with microwaves because of their aromatics and resins content. Furthermore, Porch and co-workers [19] showed, through electromagnetic simulations, that microwave heating devices for processing heavy oils could be designed and optimized to provide relatively high microwave absorption efficiencies without the need for added susceptors.

In this study, a new lab-scale microwave-heated reactor was developed and used to examine the possibility of heating THAI-produced oil directly with microwaves to 425°C in order to achieve catalytic upgrading. The system developed involves a single-mode microwave

applicator, which has the advantage of a well-defined standing wave configuration with the ability to provide high electric field intensity focused within the oil. Electromagnetic simulations were used to model and adjust the electric field configuration inside the cavity and within the heated sample.

The current study also investigates the effect of coke and sulfur deposition on the porosity and activity of the catalyst. A combination of advanced techniques including electron microscopy and computerized x-ray tomography (CXT) together with gas sorption were employed to characterize fresh and spent catalyst with the aim to: (a) study the particular pattern of coke deposition on performance, (b) investigate sulfur spatial distribution as a tracer for catalytic activity and (c) understand the effect of fabrication process of the catalyst pellets on its activity and effectiveness.

2 Materials and Methods

2.1 Materials

The heavy oil used in this study was supplied by Touchstone Exploration Inc. Canada (previously Petrobank), and was produced through THAI technology. The properties of the THAI oil used in this study are listed in Table 1.

Table 1: Properties of the THAI-produced oil used in this study

API Gravity @20 °C	Viscosity @ 25° C (cP)	Sulfur content (wt.%)
14.3	880	3.2

A commercially available mesoporous CoMo/γ-Al_2O_3 catalyst with ~ 210 m^2 g^{-1} BET surface area was used. The N_2 sorption isotherm used for surface area calculations as well as pore size distribution can be found in Section S2 and S3 in the Supporting Information document. The catalyst is a tri-lobe shaped extrudate of length ~6 mm and width ~ 1.3 mm. However,

for the microwave upgrading experiments smaller particles were used to enable homogeneous mixing of the reactor contents. The extrudates were crushed using a pestle and a mortar then divided into different particle size groups ranging from 75 µm to 1180 µm.

2.2 Experimental setup

Figure 1 is a schematic of the microwave heating system which was especially built to investigate the catalytic upgrading of the heavy oils. This system provides many advantages over similar commercially available microwave heating systems as it allows the study of a wider range of power and temperature. The reactor has a maximum operating temperature and pressure of 450 °C and 20 bar. It involves a flanged 30 mm i.d quartz tube inside a single-mode microwave applicator. The quartz tube was manufactured by Robson Scientific (Hertfordshire, UK). The quartz flange was supported and sealed against stainless steel flanges using Perfluoroelastomer (FFKM) O-rings (Polymax ltd, Hampshire, UK). A 2.45 GHz generator (GU020, IMS Ltd., Buckinghamshire, UK) with a maximum power input of 2 kW was used to supply the microwave power, which was transported to the applicator through a standard WR340 waveguide. A sliding short-circuit and a three-stub motorized Homer analyzer/tuner (STHT 2.45 GHz, S-TEAM, Bratislava, Slovakia) were used for impedance matching to improve the microwave power delivery efficiency. The sliding short-circuit enables shifting the standing wave configuration within the waveguide, while the 3-stub tuner allows for amplifying the electric field intensity in the cavity by establishing a state of resonance. The Homer analyzer/tuner also samples and analyses the microwave power signal to determine the absorbed and reflected power as well as frequency. An IR pyrometer was used to measure temperature during microwave heating (Optris CT 3MH, Berlin, Germany). The IR pyrometer operates with radiation at a wavelength of 2.3 µm, which is able to pass through the quartz wall and measure the temperature of the oil inside the tube. The reactor pressure was monitored using a pressure transducer (Omega PXM409,

Manchester, UK). A magnetic stirrer together with a glass-coated magnetic bar were used to enable mixing the reactor contents during experiments.

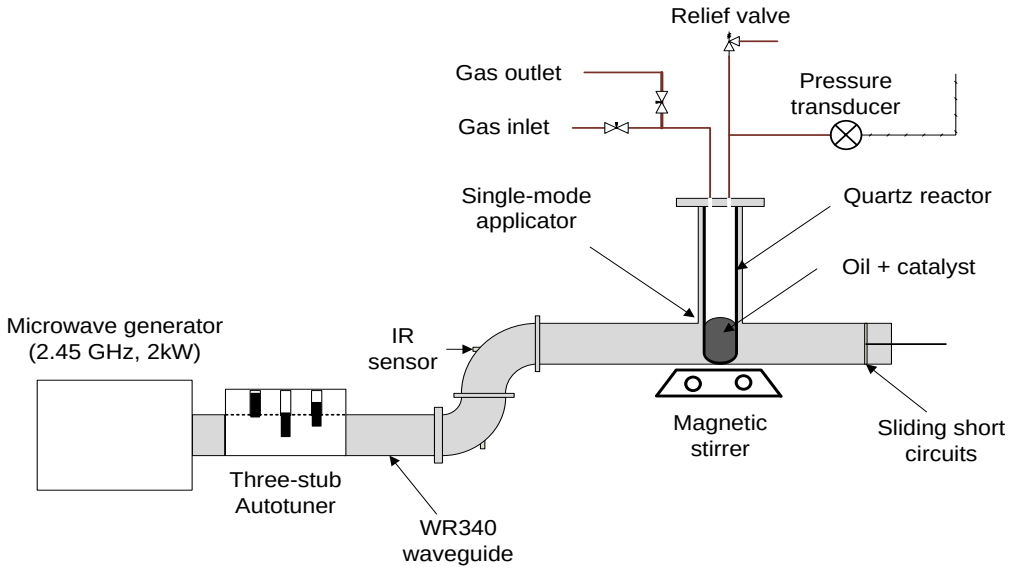

Figure 1: Schematic diagram of the laboratory-scale microwave-assisted upgrading experiment setup

In each experiment typically 15 g of oil was mixed with 1.0 g of solid catalyst in the quartz reactor. The system was then assembled as shown in Figure 1. Prior to heating the reactor was purged with nitrogen. This was performed through the pressure-swing method (CEN/TR 15281:2006) in three cycles up to 2.0 barg. The waveguide and cavity were purged continuously with nitrogen (10 L min^{-1}) during microwave heating for safety purposes in order to maintain an inert environment in case of reactor failure. The heating rate and temperature were controlled during the experiments by manually changing the microwave power input.

After heating, the reactor and its contents were left to cool down to room temperature. Before taking the reactor out of the cavity gas samples were collected in 12 mL glass sampling vials (Labco Exetainer, Lampeter, UK). The treated oil was poured into a conical centrifuge tube leaving most of the solid catalyst in the reactor. Fine particles in the oil were settled at the bottom of the tube after centrifuging at 3900 RPM for 30 minutes. The oil was then poured

into a glass vial and stored for further analysis. The spent catalyst was washed with xylene until no further color change was observed, then dried in a vacuum oven at 100 °C and stored for further analysis.

2.3 Characterization

The specific gravity of the oil was measured using a glass pycnometer according to ASTM D5355-95. The oil viscosity was measured in a cone and plate viscometer (NμLinem, ATAC, Wiltshire, UK). The sulfur content was measured using a calibrated energy-dispersive X-ray fluorescence spectrometer (Epsilon 3, PANalytical B.V, Almelo, Netherlands) following ASTM D4294-16. The dielectric properties of the heavy oil and the solid catalyst were measured using cavity perturbation techniques. Further details about the measurement procedure can be found elsewhere [14].

The composition of the gas produced after the microwave processing was determined using gas chromatography (Clarus 580 GC, PerkinElmer, Inc., US) equipped with a flame ionization detector (FID) and a thermal conductivity detector (TCD) for determination of the hydrocarbon and non-hydrocarbon gases, respectively. The obtained chromatograms were recorded and processed in an interactive software, TotalChrom (Clarus 580 GC, PerkinElmer, Inc., US).

Gas sorption analysis was carried out using a Micromeritics 3Flex instrument (Micromeritics Instrument Corp., USA). Prior to analysis, the catalyst samples were outgassed at 120 °C overnight under vacuum conditions. N_2 sorption isotherms were obtained at -196 °C. The Brunauer–Emmett–Teller (BET) model [20] was used for calculating the specific surface area. The pore size distribution was calculated using the Barrett-Joyner-Halenda (BJH) method [21]. The calculations were performed using interactive data analysis software, 3Flex analyzer V.5 (Micromeritics Instrument Corp., USA).

The coke content of the spent catalyst was determined using thermogravimetric analysis (TGA 550, TA Instruments, US). The samples were heated under air flow to 900°C at 10 °C min^{-1}, and held at 900°C for 20 min. Coke content (hard coke) was identified as the mass loss above 520 °C [22]. Sulfur deposition on the spent catalyst was determined using a sulfur analyzer (SC632, Leco Corp., USA). Scanning electron microscopy (SEM) (Quanta 600, manufactured by FEI) was used to observe the topography and granular structure of the catalyst particles. An electron microprobe (JXA-8200 EPMA, Joel), equipped with wave-dispersive spectrometry (WDS) detectors, was used to depict the spatial distribution of sulfur deposition on the spent catalyst. For electron imaging analysis, the particles were mounted in resin and polished in order to enable imaging the cross-section (center) of the particles. Computerized X-ray tomography (CXT) was used to produce high-resolution 3D images to enable observing the internal structure of the catalyst particle. The instrument used was VeraXRM-500 (Xradia Inc, Pleasanton, CA, USA).

3 Results and Discussion

3.1 Dielectric properties, electromagnetic simulations and heating profile

Figure 2 shows the loss tangent of the heavy oil and the CoMo/γ-Al_2O_3 catalyst as a function of temperature. Dielectric properties define the material's interaction with the electromagnetic field. The dielectric constant is a measure of the material's ability to be polarized and store electromagnetic energy, whilst the loss factor defines the material's ability to convert electromagnetic energy into heat. The loss tangent (tan δ), which is the ratio of the loss factor to the dielectric constant, is a measure of the efficiency of energy conversion [26]. It can be seen in Figure 2 that the loss tangent of the catalyst gradually drops with temperature up to 200 °C, above which it stays low with no significant change. This drop in the loss tangent with temperature can be attributed to the moisture evaporation as

water is considered a good microwave absorber. The loss tangent of the THAI oil, on the other hand, increases with temperature, reaching a peak at around 200 – 250°C. The increase of the loss tangent of the oil with temperature is linked to a corresponding reduction in its viscosity, whereas the drop above 250 °C is attributed to evaporation and transition in relaxation frequency [14]. The results shown in Figure 2 suggest that, above 100°C or when a dry catalyst is used microwaves will selectively heat the heavy oil in an oil-catalyst (CoMo/γ-Al_2O_3) mixture.

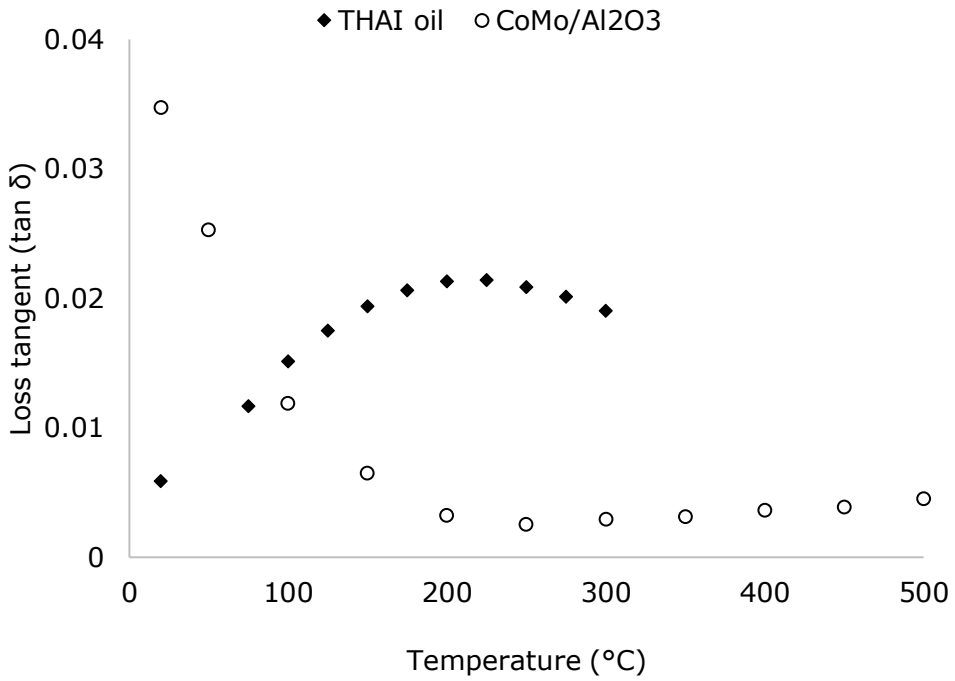

Figure 2: Dielectric loss tangent of the solid catalyst and the THAI oil. The loss tangent for the THAI oil was calculated from previous work [14].

Electromagnetic simulations using commercial software (COMSOL Multiphysics®) were performed to study the electric field distribution in the cavity and to set the sliding short-circuit at an optimized position. Further details about simulation parameters can be found in Section S1 in the Supporting Information document. Figure 3 represents an example of how the short-circuit position was adjusted to obtain the required electric field configuration in the cavity and within the sample. It displays the electric field distribution on a plane along the

center of the waveguide and the cavity, obtained from electromagnetic simulations. Figure 3 (a) shows the sliding short-circuit position that gives the highest level of microwave power conversion/dissipation. However, power dissipation in this case is achieved through two side 'hot-spots' (areas of high electric field intensity) located at the top of the oil. The short-circuit position represented by Figure 3 (b), on the other hand give an electric field configuration where one central hot-spot located near the bottom of the liquid is achieved. The short-circuit position represented by Figure 3 (b) was chosen because it focuses the field near the center of the liquid where the catalyst particles are more likely to be present, even though it achieves smaller absorbed power compared to the position represented by Figure 3 (a) (45% lower).

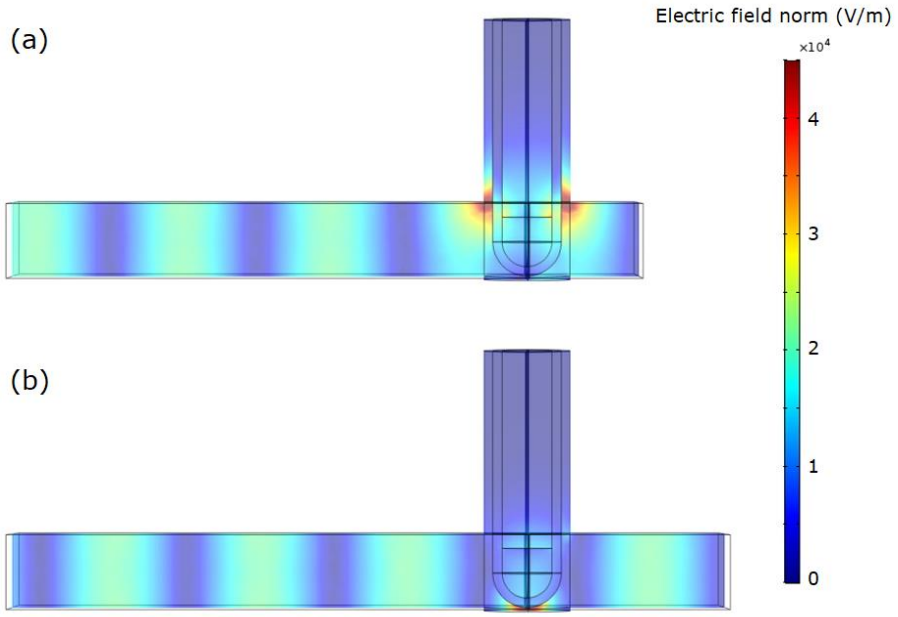

Figure 3: Simulated electric field distribution in the cavity with the sliding-short circuit set to focus the field at the sample: (a) the sliding-short position is 6.5 cm from the center of the cavity resulting in 5.5 % absorbed power; (b) the sliding-short position is 11.0 cm from the center of the cavity resulting in 3 % absorbed power. It should be noted that this does not include the effect of the three-stub tuner which amplifies the electric field intensity and, thus, increases the absorbed power.

The effect of the short-circuit position and, thus, the location of hot-spots on the heating profile was tested experimentally. Figure 4 displays power, temperature and pressure profiles

during microwave heating experiments, which were run using the corresponding sliding-short position in Figure 3. The profile in Figure 4 (a) which was obtained using the short-circuit position in Figure 3(a) (case a) resulted in 1.02 increase in the API, whereas the profile in Figure 4 (b) which was obtained using the short-circuit position in Figure 3(b) (case b) resulting in 2.47 increase in the API. It can be noted from Figure 4 that case (b) needed higher power to reach and maintain the same temperature compared to case (a). The variations in the power requirement and API gravity between the two cases, despite having the same holding temperature, can be explained by the variations in the electric field configuration shown in Figure 3. The side hot-spots in Figure 3 (a) resulted in higher temperature near the surface than at the center. Since the IR pyrometer measures surface temperature, then the temperature at the center of the sample and thus the average temperature in case (b) would be higher than that in case (a) resulting in higher absorbed power and greater API gravity.

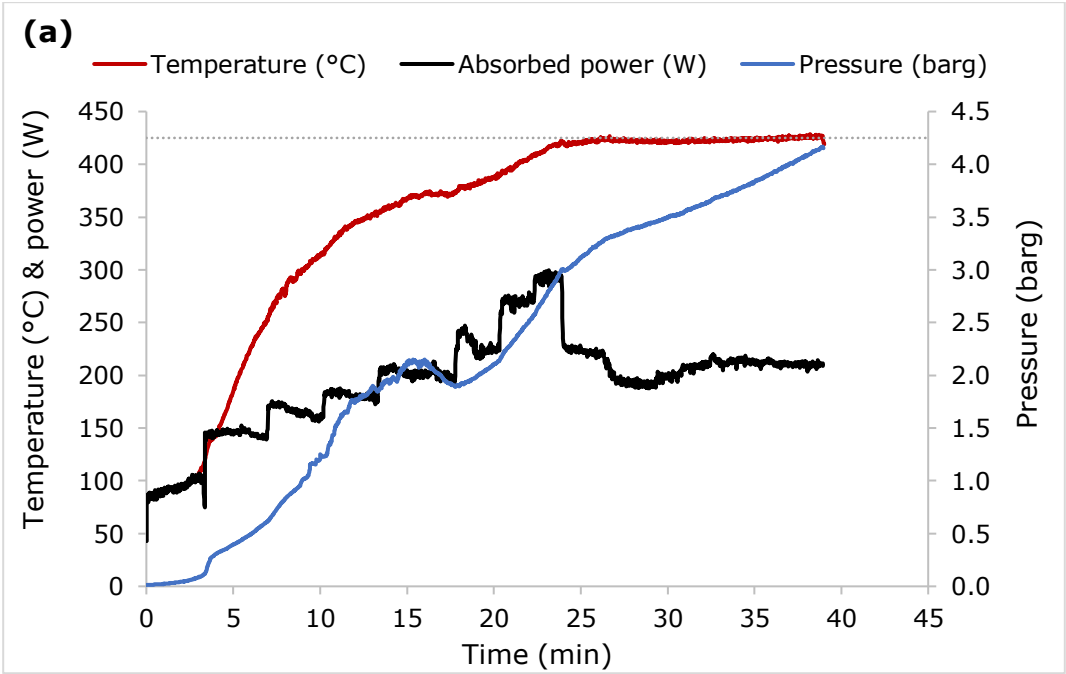

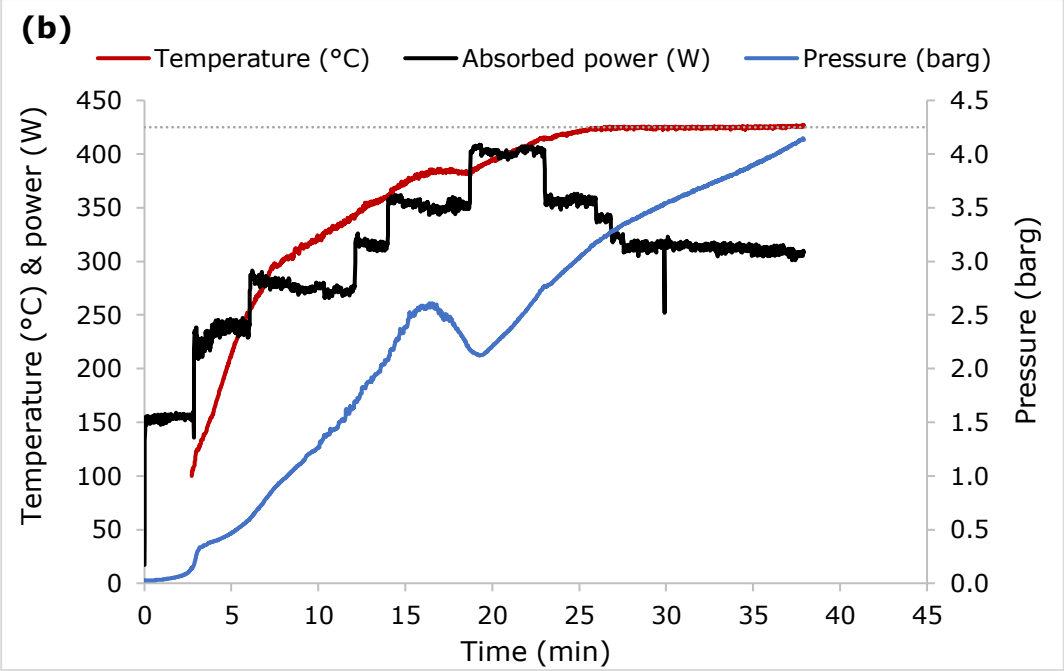

Figure 4: Typical profiles during microwave heating of THAI oil: (a) obtained using the short-circuit position represented by Figure 3(a) resulting in 1.02 increase in the API; (b) obtained using the short-circuit position represented by Figure 3(b) resulting in 2.47 increase in the API.

Figure 4 shows that under the applied power profile it was possible to heat the heavy oil to the target temperature of 425 °C in about 30 minutes. Heating in the range between 100 °C to 300 °C is the fastest. The slowing-down rate above 300 °C can be attributed to the boiling/condensation cycles of the lighter fractions within the oil. This leads to power which would otherwise be consumed in increasing oil temperature (sensible heat) to supply the latent heat of vaporization as well as compensating for heat lost to the cooling jacket at the top of the reactor. The results shown in Figure 4 demonstrate, contrary to previous assertions that heavy oil can be heated to such high temperatures with no need for an additional microwave susceptor.

3.2 Catalytic upgrading and catalyst activity

A series of batch microwave heating experiments were run to evaluate the degree of upgrading at 425°C. Figure 5 shows the effect of holding time on the degree of upgrading and

desulfurization using catalyst with a particle sizes in the range 212 – 600 μm. As can be seen in Figure 5 (a) the API gravity increases with time up to 15 minutes, beyond which no significant increase is realized. A similar plateau is reached for the viscosity which drops with the holding time to less than 100 cP. This decaying rate of increase in the levels of upgrading after 15 minute holding time can be attributed to catalyst deactivation due to pore blockage and loss of activity as will be discussed in further detail later in this paper. As can be seen in Figure 5 (b), the increase in API gravity and reduction of viscosity is coupled with desulfurization of the treated oil and an increase in sulfur deposition on the solid catalyst. The rate of oil desulfurization starts to decrease after 15 minute holding time due to catalyst deactivation.

It is to be noted here that sulfur deposition on the solid catalyst could be useful. Sulfided CoMo catalysts have better HDS activity compared to unsulfided catalysts [23]. One of the strategies for sulfidation of HDS catalysts is heating them in sulfur-containing hydrocarbons [23], which is what is thought to be happening here with the sulfur deposition. However, as will become apparent below, there are two competing factors affecting the activity of the catalyst in the current situation. The first is the increase in the degree of sulfidation, which improves the catalyst activity, and the second is the pore blockage due to coke deposition, which makes the active sites inaccessible by the reactants.

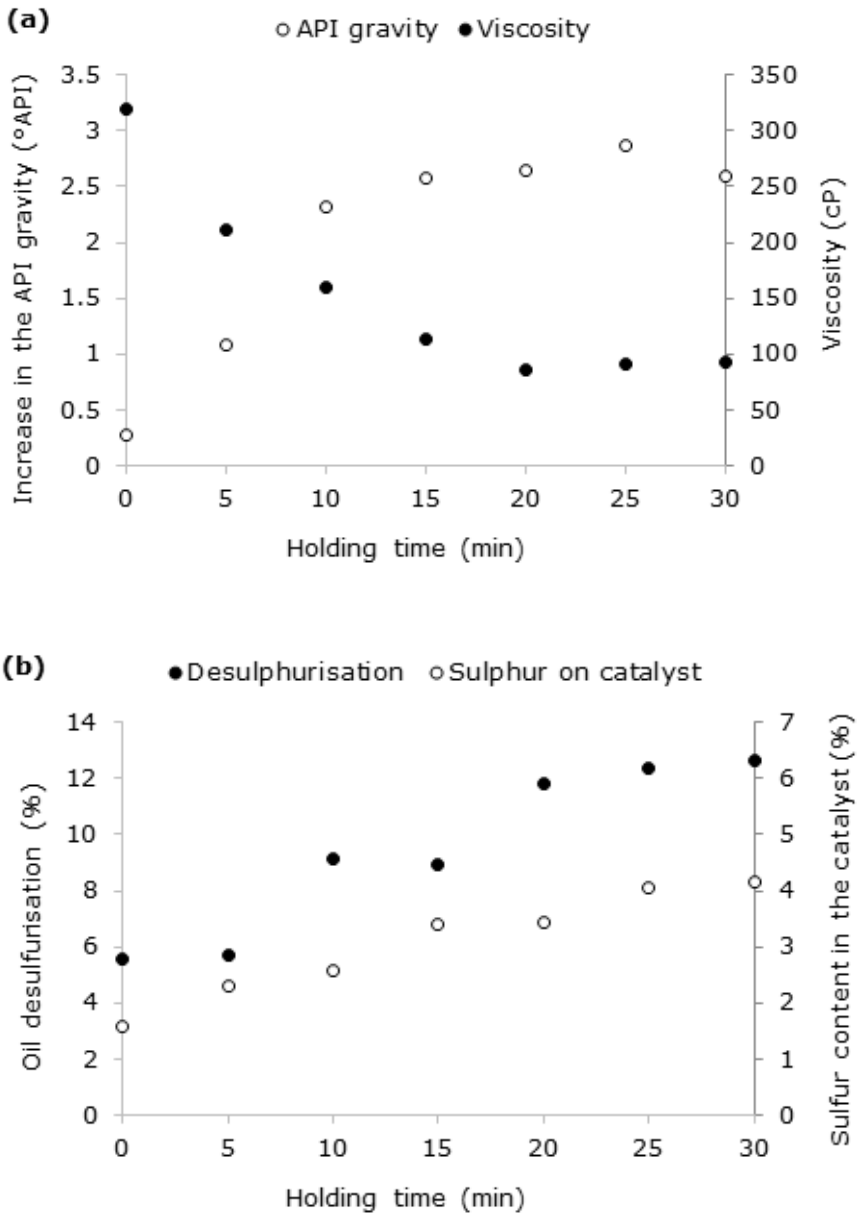

Figure 5: Effect of holding time at 425 °C on (a) API gravity & viscosity, and (b) sulfur content. Experiments were run using CoMo/γ-Al_2O_3 catalyst with 212 – 600 µm particle size. Catalyst = 1.0 g, oil = 15 g.

The catalytic activity of the CoMo/γ-Al_2O_3 was evaluated and compared to that of only a γ-Al_2O_3 support. Table 2 displays results obtained under similar conditions for the two cases at 425 °C and 15 min holding time. It can be seen that γ-Al_2O_3 achieves higher API gravity and lower viscosity compared to the CoMo/γ-Al_2O_3 catalyst. The use of alumina alone leads to greater cracking, resulting in production of high naphtha fraction, which is the reason for the observed low viscosity in the upgraded oil. However, the CoMo/γ-Al_2O_3 catalyst provides

higher desulfurization. Table 2 also shows variations in the gas composition indicating variations in the process chemistry between the two cases. The gas composition arising from use of the γ-Al_2O_3 is a typical product of thermal cracking while that arising from use of CoMo/γ-Al_2O_3 is typical of the composition of gases originating from catalytic cracking (acid-activated) [24]. In general, thermal cracking gives high yields of C_1 and C_2 gases (methane, ethane and ethylene), whereas C_3- C_6 are the major light hydrocarbon products in catalytic cracking [24].

Table 2: Comparison of the performance of CoMo/γ-Al_2O_3 to that of γ-Al_2O_3. Experiments were run under similar conditions at 425 °C and 15 min holding time with particles of 212 – 600 µm size.

	CoMo/γ-Al_2O_3	γ-Al_2O_3
Increase in API	2.58 ± 0.14	3.03 ± 0.06
Viscosity (cP)	114.1 ± 1.16	86.50 ± 7.71
Reduction in sulfur (%)	8.90 ± 0.41	6.71 ± 0.35
Sulfur deposition on solid (%)	3.38 ± 0.12	0.70 ± 0.06
Gas composition (mole %)		
Methane	0.018	12.792
Ethane	0.013	5.753
Ethene	0.000	1.226
Propane	0.013	4.139
Propene	0.007	2.436
Butane	0.005	0.000
Butene	0.002	0.633
Pentane	0.003	0.500
Pentene	0.015	0.427
Hydrogen	18.879	0.779
Carbon dioxide	0.632	1.036
Carbon monoxide	0.790	1.065
Hydrogen sulfide	6.782	11.896

Table 2 also shows considerably higher hydrogen in the CoMo/γ-Al_2O_3 produced gas compared to γ-Al_2O_3. Hart and co-workers [25] have recently shown that in an inert atmosphere (nitrogen), CoMo/γ-Al_2O_3 induces dehydrogenation, whereas, under a hydrogen

atmosphere it catalyzes hydrogenation. This induced dehydrogenation by CoMo/γ-Al_2O_3, which leads to the production of unsaturated compounds explains the lower API compared to γ-Al_2O_3. Hydrogen production during the catalytic upgrading involves complex reactions such as catalytic dehydrogenation of naphthenes (i.e., cycloalkanes) and aliphatic hydrocarbons into aromatic and olefins. This can be confirmed from the release of olefinic gases such as ethene, propene, butene, etc in the gaseous product presented in Table 2. Also, the catalytic cleavage of hydrocarbon C – H bonds by the Co and Mo active and promoter metals of the catalyst could have been the major mechanism of hydrogen release as shown in Table 2. This is because despite the higher olefin content of the gas produced when γ-Al_2O_3 is used; the hydrogen produced by CoMo/γ-Al_2O_3 catalyst is higher. It can also be noted from Table 2 that CoMo/γ-Al_2O_3 produced less hydrogen sulfide than γ-Al_2O_3. However, more sulfur is deposited on the CoMo/γ-Al_2O_3 catalyst. Indeed, nearly 90% of the sulfur removed from the oil when CoMo/γ-Al_2O_3 was used was deposited on the catalyst.

Although CoMo/γ-Al_2O_3 has been found to be more active in desulfurization, hydrogen may need to be added to the system in order to suppress dehydrogenation occurring concurrently. This consequently limits upgrading in terms of API gravity and viscosity. In addition to its ability to improve the API gravity and reduce viscosity, hydrogen has been previously shown to reduce coke formation and deposition on the catalyst [26]. Injecting and delivering hydrogen to the catalyst packing in the reservoir could be a challenging and costly task. However, a possible alternative is to produce hydrogen in-situ. Adding a hydrogen donor such as cyclohexane, decalin or tetralin has been previously suggested to generate hydrogen in-situ [15, 22]. A novel, alternative could be to exploit part of the oil-in-place itself as a hydrogen donor. It has been demonstrated that CoMo/γ-Al_2O_3 is capable of dehydrogenating the heavy oil, producing nearly 20% hydrogen in the gas product as shown in Table 2. It is therefore suggested that part of the oil-in-place could be targeted for ‘deep’ dehydrogenation.

The produced hydrogen could then be directed to aid hydrodesulfurization and improve the upgrading. This concept is equivalent to in-situ combustion where part of the oil is sacrificed in combustion to produce the heat needed to mobilize the rest of the oil-in-place [7]. Further, this could provide a new route for hydrogen production from oil reservoirs which can be used for chemicals synthesis and clean energy production and contribute to the efforts towards a hydrogen economy.

3.3 Effect of particle size and coke deposition on upgrading and catalyst activity

The effect of coke deposition on the catalyst porosity and activity was further investigated. Compared to conventional oil and lighter hydrocarbons, heavy oils have a higher tendency to producing coke during thermal treatment, which can lead to pore blockage and loss of activity when deposited on the catalyst. Hence, a combination of advanced techniques were employed to characterize fresh and spent catalyst samples.

Figure 6 displays the effect of particle size on the catalytic activity and the catalyst performance. Figure 6 (a) shows that using smaller particles leads to better upgrading, i.e. higher API, lower viscosity and higher desulfurization. Upgrading with up to ~3.2° increase in API, ~90% reduction in viscosity to less than 100 cP, and ~12% reduction in sulfur content (desulfurization) is achieved when 75-106 µm particles were used. Figure 6 (b) shows that coke and sulfur deposition on the spent catalyst is higher for smaller particles, which is in line the catalytic activity and improvement in the degree of upgrading noted from Figure 6 (a). However, as can be seen in Figure 6 (b), larger particles demonstrate lower surface area despite their lower catalytic activity and smaller coke deposition. This indicates that most of the coke deposition happens on the outer layers of the catalyst particle. In general, the spent catalyst has experienced more than 60% drop in the BET surface area, which is believed to be caused primarily by coke deposition.

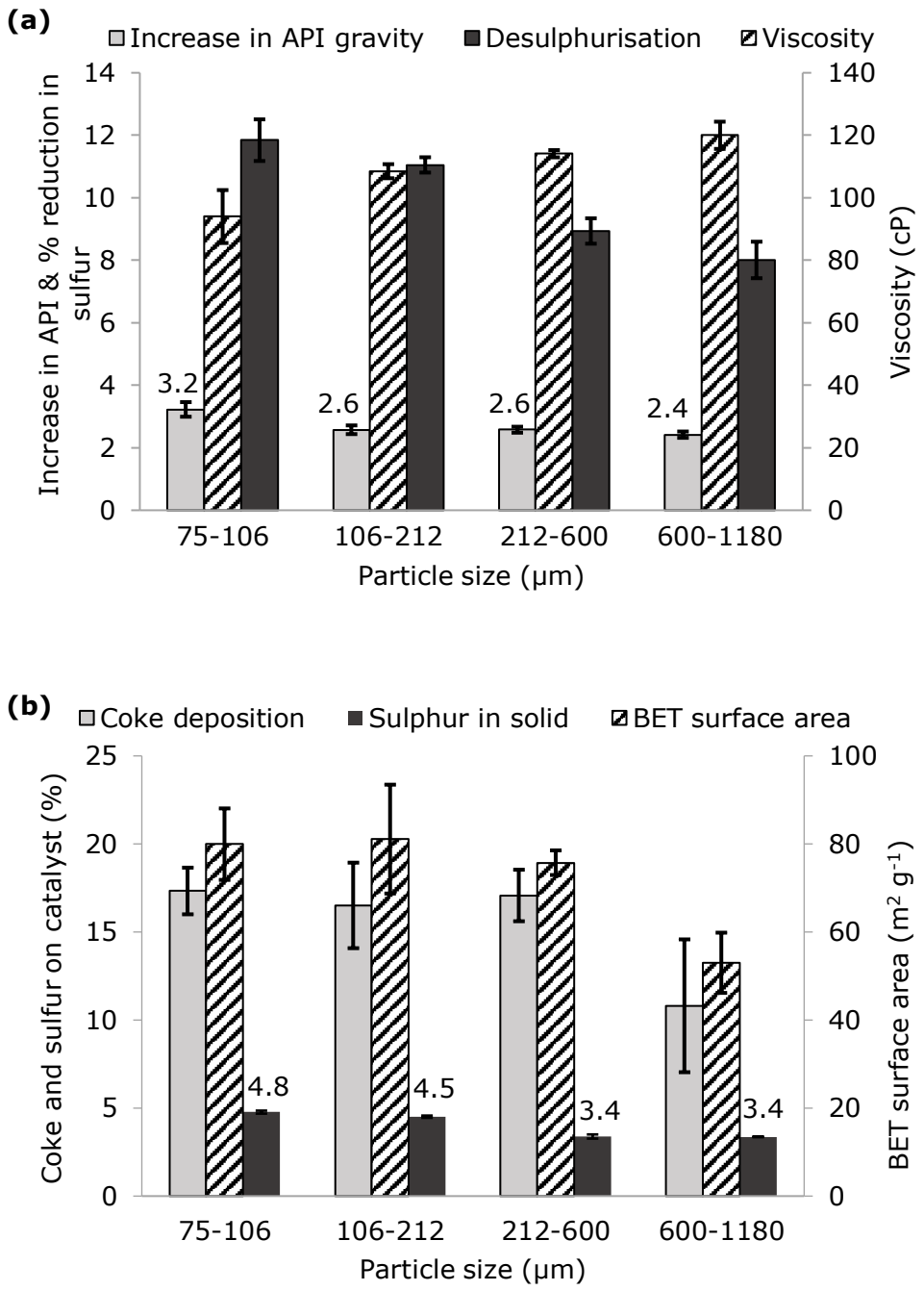

Figure 6: Effect of particle size on: (a) API gravity, viscosity & desulfurization; and (b) coke and sulfur deposition, and BET surface area of the spent catalyst. Results are at 425 °C and 15 minutes holding time

Electron microscopy was used to image the spatial distribution of sulfur deposition on the catalyst particle as a tracer of catalytic activity within a catalyst particle. Figure 7 shows that sulfur deposition on the outer layers of the catalyst particle is higher than in the center. This is in agreement with what has been noted from the results in Figure 6, as both suggest higher

catalytic activity on the outer layers of the catalyst particle, which is an indication that the upgrading and desulfurization process in the current situation is a diffusion-limited process.

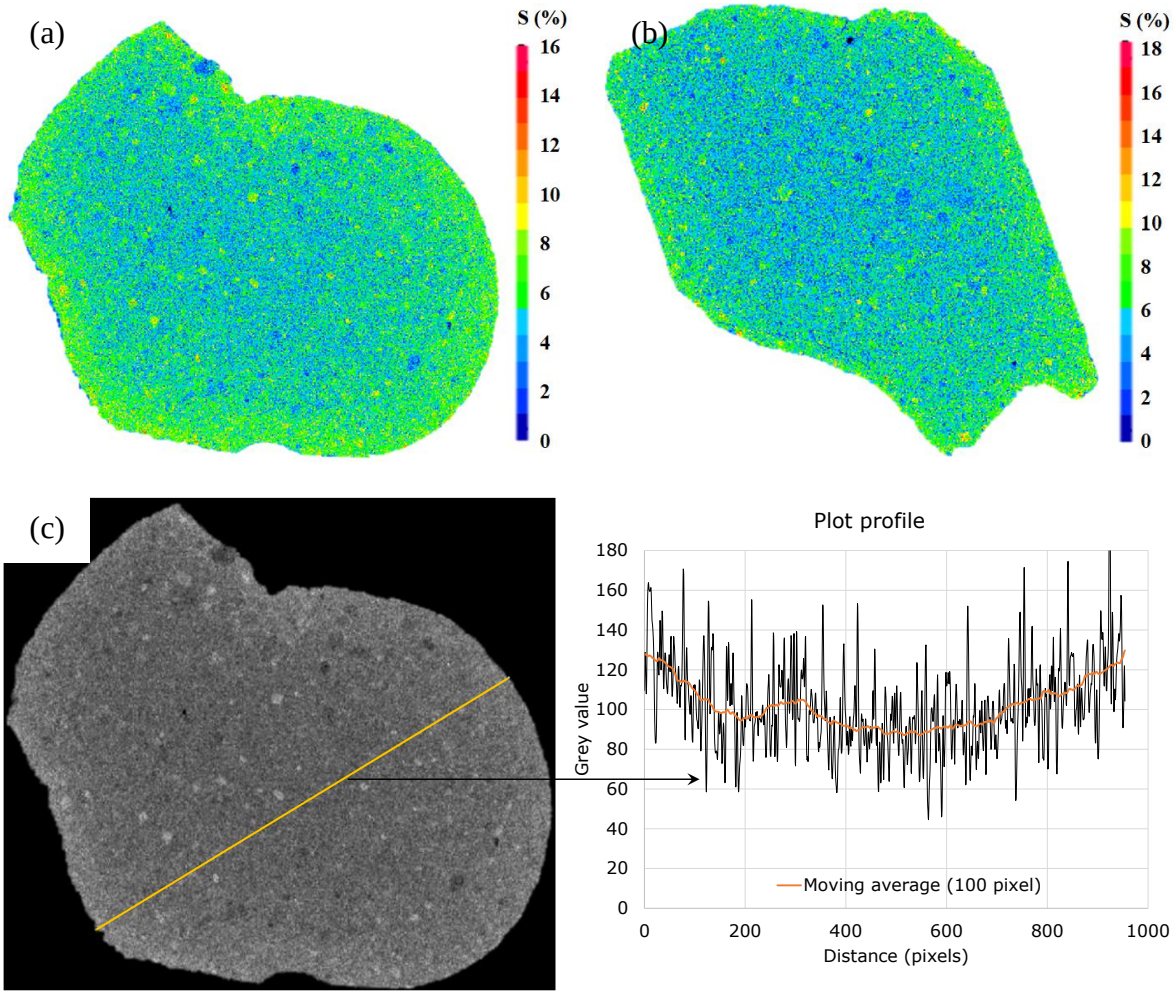

Figure 7: Spatial distribution of sulfur deposition on the catalyst (600 - 1180 µm) after 15 minutes holding time at 425°C. (a) and (b) display sulfur concentration map of two different samples, (c) shows a plot profile of a line across the surface of the sample in (a). The profile was obtained using an image processing software (ImageJ developed by NIH, USA)

The relationship between the intra-particle diffusion and rate of reaction in porous catalysts is commonly explained and quantified through the Thiele Modulus, ϕ, which is a measure of the ratio of reaction rate to diffusion rate [27, 28]. When ϕ is large internal diffusion controls the overall rate and reactions take place mainly on the external surface of the catalyst. When ϕ is small the whole catalyst particle is involved in the reactions with a larger degree of

homogeneity. The catalytic process in such a case is rate-limited. Based on the electron imaging displayed in Figure 7 and the discussion on the relationship between coke deposition and surface area, it can be concluded that the catalytic process in the current study is diffusion-limited with a finite high ϕ value.

In addition to the general pattern, of a higher concentration in the outer layers, sulfur deposition shows other forms of spatial heterogeneity, including fingering/branching patterns, and the presence of patches/spots of high sulfur content within, otherwise, low sulfur regions, and vice versa. Computerized X-ray tomography (CXT) was used to help in understanding these forms of heterogeneity in sulfur spatial distribution. Figure 8 displays a 2D cross-section through 3D reconstructed CXT images of fresh CoMo/γ-Al_2O_3 catalyst. The contrast in CXT images reflects variations in electron density, with brighter pixels indicating heavier elements and darker pixels indicating either lighter elements or lower density [29]. Hence, the dark-grey background in Figure 8 represents empty-space (air). It can be noticed in Figure 8, as well as the SEM micrograph in Figure 9, that the catalyst particles have a granular appearance, which is probably due to the powder nature of the feed used for making the catalyst extrudates. Figure 9 displays that some of the grains forming the catalyst particle have higher density (i.e. less porous) than others. This granular nature can explain the aforementioned heterogeneity in sulfur spatial distribution, specifically the fingering/branching pattern that is probably caused by reactants avoiding dense (less porous) grains. As the reaction is believed to be diffusion-limited, then the flux of reactants passing though the catalyst particle would tend to avoid these less porous grains.

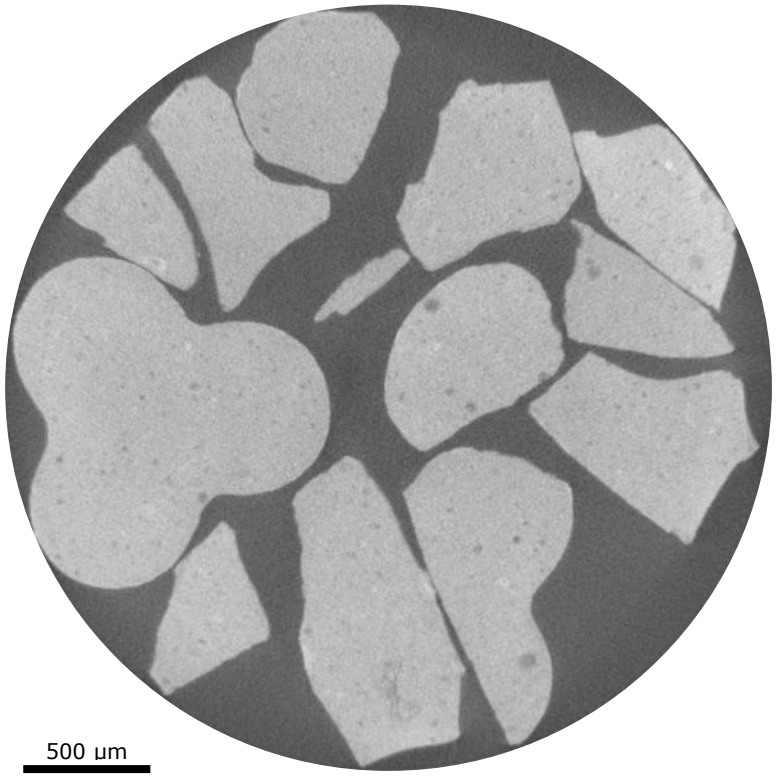

Figure 8: 2D cross-section through 3D reconstructed CXT images of fresh CoMo/γ-Al_2O_3 catalyst. Voxel resolution of 5.0 µm was used.

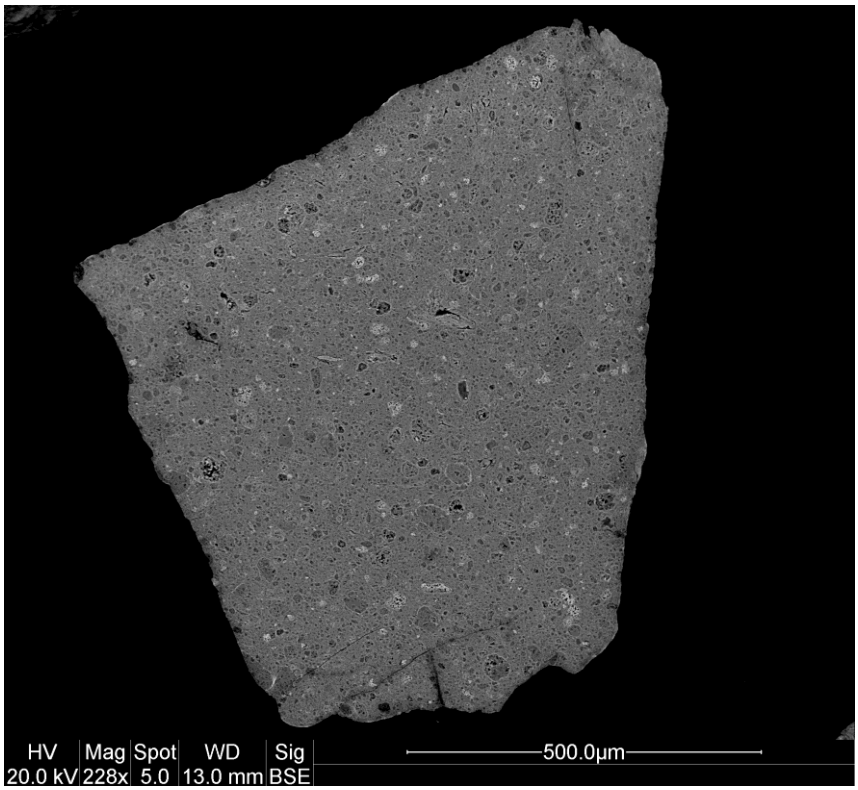

Figure 9: SEM (backscattered-electron) image for a spent catalyst particle showing, more clearly, the granular appearance of the catalyst particles with some grains being less dense (more porous) than others.

It can also be observed in Figure 8 that the fresh catalyst contains some dark patches as well as some bright (white) spots. The dark patches represent areas of air gap within the catalyst or highly porous (less dense) grains as can be seen more clearly in Figure 9, whereas the bright spots are likely locations of high concentration of the metal catalyst (Co and Mo). Correspondingly, it can be seen in Figure 7 that there are discrete blue spots (low S content) distributed across the surface including the outer layers which are, generally, areas of high sulfur content. These discrete blue spots can be explained as being empty-space equivalent to the dark patches in the CXT image. Similarly, the discrete yellow and orange spots (high S content), which are randomly distributed across the surface including the center in Figure 7 can be linked to the areas of high metal concentration (bright spots) in the CXT image. During sulfidation of HDS catalysts, sulfur interacts with the metal catalyst (specifically Mo) forming metal sulfides (MoS_2) [23, 30]. This explains the high sulfur content at the areas of high metal concentration. Examples of spots of high sulfur concentration matching areas of high metal concentration can be seen in the electron microscopy images shown in Section S4 in the Supporting Information document.

It can be concluded from the previous discussion that the heterogeneity in the sulfur spatial distribution can be attributed in part to the fabrication process of the catalyst pellets/extrudates (granular form) as well as the uneven metal-catalyst dispersion. It is to be noted that the pore sizes in the catalyst are below the resolution currently possible to image directly with hard x-ray tomography [31, 32] and the sample volumes it is possible to probe by electron microscopy are statistically unrepresentative in this case, and therefore gas adsorption was used to further characterize the pore structure.

Figure 10 displays N_2 isotherms of fresh and spent catalysts. A sharp increase in the gas uptake at low pressure can be seen in the case of fresh catalyst, which indicates the presence

of micropores. However, the spent catalysts do not have the same sharp increase at low relative pressure, which suggests that the majority of the micropores have been filled, or their access blocked, with coke. This was confirmed by fitting the isotherms to a two-component, homotattic patch model with a Langmuir component to represent micropore adsorption and a BET component to represent mesopore multi-layer adsorption [33]. The micropore volume was then calculated from the Langmuir adsorption capacity parameter, and the fraction of the surface represented by the Langmuir model. The fitted curves and parameters can be found in Section S5 in the Supporting Information document. It was found that the spent catalysts experienced over 70% reduction in their micropore volume based on that of the fresh catalyst. The pore size distributions displayed in Figure S3 (b) in the Supporting Information document also show reduction in pore sizes of spent catalyst relative to the fresh catalyst.

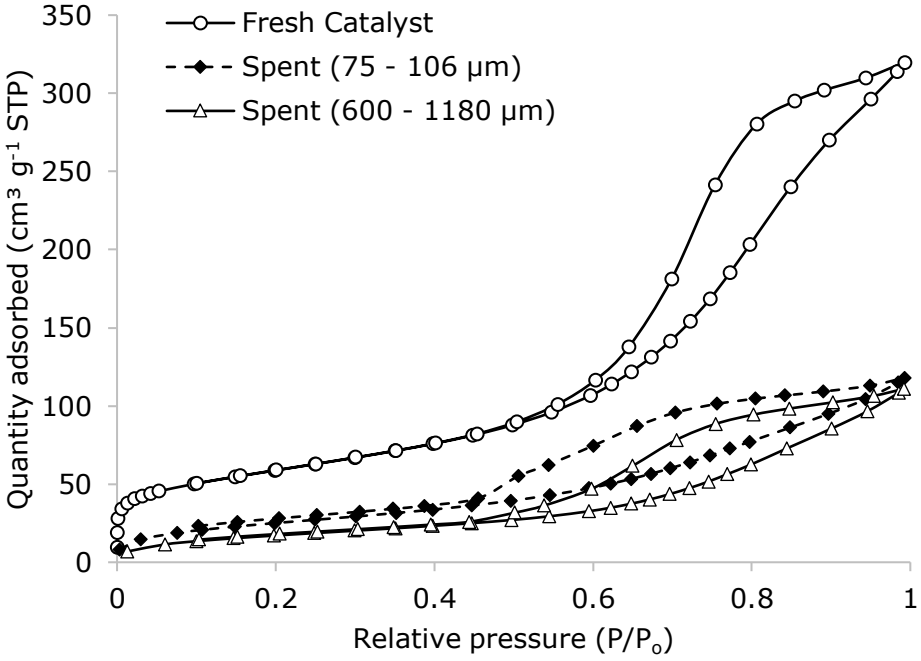

Figure 10: N_2 sorption isotherms for the fresh and spent catalyst

In addition to the drop in total gas uptake for the spent catalyst compared to the fresh catalysts, which is reflected in losses in pore size and volume and surface area, it can be noted in Figure 10 that there is an increase in the width of the sorption hysteresis in the case

of spent catalysts. In a disordered interconnected pore network the width of the hysteresis is an indication of the pore network conductivity where narrower width of a hysteresis suggests high pore network connectivity and vice versa. Seaton and co-workers [34-36] have applied percolation theory to model pore network connectivity from gas sorption isotherms. In percolation theory, the mean coordination number, Z, is used as a measure for network connectivity. Larger Z indicates higher pore network connectivity, which should result in smaller (narrower) hysteresis width, and vice versa.

Percolation theory was applied to the N_2 sorption isotherms of the fresh and spent catalyst samples. The fitting data can be found in Section S6 in the Supporting Information document. It can be seen from Table 3 that the mean coordination number of the spent catalysts are smaller than that of the fresh catalyst. This indicates that the pore network conductivity decreased due to blockage in the pathways. The higher decrease in the pore network connectivity in the case of the smaller particles can be linked to their higher coke deposition.

Table 3: values for coordination number obtained after applying percolation theory on N_2 sorption isotherms

Sample	Fresh catalyst	Spent catalyst			
		600 - 1180 µm	212 - 600 µm	106 - 212 µm	75 - 106 µm
Z	8.6	5.8	5.6	4.9	4.8

It has been found that, while larger catalyst particles have lower production and laydown of coke and sulfur, they lose more accessible surface area. The gas sorption isotherms suggest that narrow pore necks are retained for smaller particle sizes despite the increased coke production. This apparently counter-intuitive set of findings described above can be understood coherently within the context of the model shown schematically in Figure 11. The pore structure of whole catalyst pellets, and fragments of large particle size, can be considered to be like a through ink-bottle pore, whereby larger pore bodies are shielded at both ends by narrower pore necks. This structure is analogous to the large voids surrounded

by porous solid matrix visible in the electron microscopy image in Figure 9. The gas sorption hysteresis suggests similar types of structure will also probably exist for smaller pore sizes not directly visible in the image. In the model, the surface of the pores may have microporous roughness that accounts for the loss of microporosity observed. It is further supposed that the reactions for the production of coke and sulfur are diffusion-limited, and thus the spatial pattern of overall coke and sulfur laydown will be pore-mouth-plugging dominated, such that the solid deposition has the wedge-shaped profile shown schematically in Figure 11 [37]. This is consistent with the general pattern of decreasing sulfur concentration along a particle diameter, moving from the surface towards the center of the particle, as seen in the sulfur map given in Figure 7. In the case of large particles, the pore necks will tend towards plugging after only a relatively low amount of solid deposition, and that small amount of solid will block off access to a relatively large surface area. However, for smaller particle sizes, the greater fragmentation may have removed the pore shielding represented by one of the narrow necks in the model. Hence, larger pore bodies would become more accessible. The exposed larger pores would be more resistant to plugging, and allow easier diffusion, which would mean that more reaction could take place deeper within the particles. This means more surface area remains accessible despite greater coke laydown. If, as shown in Figure 11 (b), the thinner end of the coking wedge extended to the interior side of the remaining pore necks, even smaller necks might then be formed, but still remain accessible. This effect may have given rise to the appearance of a second desorption (cavitation) knee at lower relative pressure in the sorption isotherms for the smaller particles in Figure S2 (Supporting Information document), where little, or no, desorption was apparent before for larger particles. This feature of the model demonstrates the deep level of overall penetration of the coke wedge. The pore connectivity from percolation analysis is a proxy measure of the

width of the hysteresis loop, and the lower connectivity for smaller particles may reflect the broadening in the hysteresis this effect creates.

This model and the imaging results highlight the need to manufacture a catalyst particle with more uniform larger pore sizes, and avoiding shielding, perhaps by ensuring powder feed particles are lower, and have less variability, in density.

(a) Large particle size

(b) Small particle size

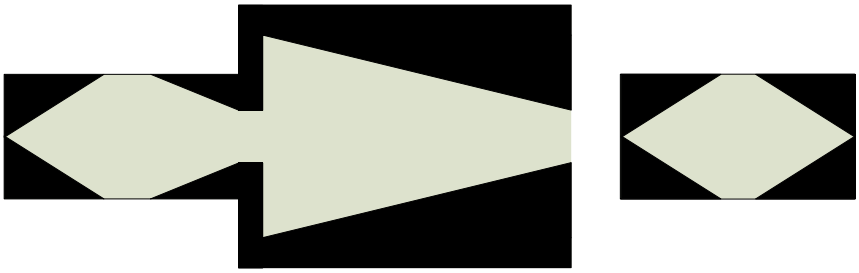

Figure 11: Proposed pore model showing larger particles having a through ink-bottle structure with larger pore bodies shielded at both ends by narrower pore necks as shown in (a). For small particles, fragmentation may remove the pore shielding as displayed in (b).

In summary, coke deposition and its effect on the activity of HDS catalysts remains one of the challenges that requires further research, especially when dealing with heavy oils. One of the options to improve intra-particle diffusion and avoid coke deposition on the external layers is either using smaller catalyst particles and/or engineering catalysts with more uniform larger pore sizes as mentioned earlier. However, both options could have their drawbacks, as using smaller catalyst particles could lead to particles entrained by the oil and results in separation difficulties, whereas using larger pores could reduce the specific surface

area of the catalyst. Hydrogen has also been shown previously to reduce coke formation and deposition on the catalyst [26] in addition to its contribution in improving upgrading and desulfurization activity. However, as discussed earlier, delivering hydrogen into the reservoir could be a challenging and costly task, and further work is needed to investigate in-situ generation of hydrogen.

4 Conclusions

This study examined targeted microwave-heating as a strategy to provide additional heating in the THAI-CAPRI process to achieve successful catalytic upgrading. It was demonstrated that temperatures up to 425 °C could be achieved with no need for adding a supplemental microwave susceptor. Upgrading with more than 3.2° increase in API gravity, a reduction in viscosity to less than 100 cP, and more than 12% reduction in sulfur content was achieved using commercially available CoMo/γ-Al_2O_3 catalyst.

Although, CoMo/γ-Al_2O_3 was found to be more active in desulfurization compared to γ-Al_2O_3, it induced dehydrogenation leading to a lower increase in API gravity and reduction in viscosity. It was suggested that, in THAI-CAPRI field settings, part of the oil-in-place could be sacrificed and targeted for deep dehydrogenation. The produced hydrogen could be then directed to aid hydrodesulfurization and improve the upgrading. Increased hydrogen in produced gases can also be separated at the surface for use elsewhere.

Analysis of fresh and spent catalyst showed that coke deposition happens on the outer layers of the catalyst particle. In addition to the general loss in the pore volume and surface area, coke deposition blocked access to the majority of the micropore volume and reduced pore network connectivity which had existed in the fresh catalyst.

The relative rate of the coking reaction compared to mass transport, manifested in the pattern of coke laydown, meant that the two solid deposition reactions were in competition, since the desulfurization (and upgrading) has also been shown to be diffusion-limited.

Based on development with time on-stream of a unusual second desorption step in the gas sorption isotherm data together with observations from coke and sulfur deposition, an evolving pore structural model was proposed. The model involved an initial through ink-bottle structure, whereby larger pore bodies are shielded at both ends by narrower pore necks, except in smaller particles where this shielding was removed by fragmentation. The subsequent spatial pattern of overall coke and sulfur laydown in this model was pore-mouth-plugging dominated, such that the solid deposition created a wedge-shaped profile that explained the various characterization data for both large and small catalyst particles. In addition, the imaging results highlighted the inter-action between the sulfidation process and the particular type of heterogeneities introduced by the specific pellet forming process, and thereby showed the need to manufacture a catalyst particle via a method providing more uniform larger pore sizes.

This study demonstrated that microwave heating technique is a viable option for providing the targeted additional heating needed for successful in-situ catalytic upgrading in field-scale THAI-CAPRI settings. However, further research is needed to tackle the challenges around hydrogen provision for better upgrading and desulfurization as well as controlling pore blockage due to coke deposition.

Acknowledgements

The authors would like to thank Petrobank Energy and Resources, Ltd. (now Touchstone Exploration Inc.), Canada for supplying the oils used in this study. We would like also to thanks Dr Clement Uguna and Adrian Quinn from the Low Carbon Energies and Resources

(LCERT) Research Group at University of Nottingham (UoN) for their help with gas and sulfur analysis; Dr Aleksandra Gonciaruk from the GeoEnergy Research Centre (UoN) for her help with gas sorption experiments; Dr Elisabeth Steer from the Nanoscale and Microscale Research Centre (nmRC) (UoN) for her assistance with electron imaging; and Dr Martin Corfield from the Power Electronics, Machines and Control Group (UoN) for his assistance with the CXT imaging.

Funding: This work was supported by the Engineering and Physical Sciences Research Council [grant number EP/N032985/1]

References

[1] EIA, *International Energy Outlook 2019 with Projections to 2050*. 2019, U.S. Energy Information Administration: Washington, DC.
[2] Bui, M., et al., *Carbon capture and storage (CCS): the way forward.* Energy Environ Sci, 2018. **11**(5): p. 1062-1176 DOI: 10.1039/C7EE02342A.
[3] IEA, *The Future of Petrochemicals: towards more sustainable plastics and fertilisers (executive summary)*. 2018, International Energy Agency
[4] Gates, I.D. and J. Wang, *In-situ process to produce hydrogen from underground hydrocarbon reservoirs.* 2017. W.I.P. Organization, WO/2017/136924
[5] Bata, T., et al., *AAPG Energy Minerals Division Bitumen and Heavy Oil Committee Annual Commodity Report-May 2019.*
[6] Hein, F.J., *Geology of bitumen and heavy oil: An overview.* Journal of Petroleum Science and Engineering, 2017. **154**: p. 551-563 DOI: https://doi.org/10.1016/j.petrol.2016.11.025.
[7] Shah, A., et al., *A review of novel techniques for heavy oil and bitumen extraction and upgrading.* Energy Environ Sci, 2010. **3**(6): p. 700-714 DOI: 10.1039/B918960B.
[8] Guo, K., H. Li, and Z. Yu, *In-situ heavy and extra-heavy oil recovery: A review.* Fuel, 2016. **185**: p. 886-902 DOI: http://dx.doi.org/10.1016/j.fuel.2016.08.047.
[9] Xia, T.X., et al., *THAI—A 'Short-Distance Displacement' In Situ Combustion Process for the Recovery and Upgrading of Heavy Oil.* Chem Eng Res Des, 2003. **81**(3): p. 295-304 DOI: https://doi.org/10.1205/02638760360596847.
[10] Shah, A., et al., *Experimental Optimization of Catalytic Process In Situ for Heavy-Oil and Bitumen Upgrading.* J Can Pet Technol, 2011. **50**(11-12): p. 33-47 DOI: 10.2118/136870-PA.
[11] Xia, T. and M. Greaves, *3-D Physical Model Studies of Downhole Catalytic Upgrading of Wolf Lake Heavy Oil Using THAI*, in *Canadian International Petroleum Conference*. 2001, Petroleum Society of Canada: Calgary, Alberta. p. 15.
[12] Rabiu Ado, M., M. Greaves, and S.P. Rigby, *Dynamic Simulation of the Toe-to-Heel Air Injection Heavy Oil Recovery Process.* Energy Fuels, 2017. **31**(2): p. 1276-1284 DOI: 10.1021/acs.energyfuels.6b02559.

[13] Adam, M., et al., *Microwave-assisted Catalytic Upgrading of Heavy Oil*, in *4th North American Symposium for Chemical Reaction Engineering (NASCRE 4)*. 2019: Houston, Texas.
[14] Zhang, Y., et al., *Impact of Oil Composition on Microwave Heating Behavior of Heavy Oils.* Energy & Fuels, 2018. **32**(2): p. 1592-1599 DOI: 10.1021/acs.energyfuels.7b03675.
[15] Hart, A., et al., *Tetralin and Decalin H-Donor Effect on Catalytic Upgrading of Heavy Oil Inductively Heated with Steel Balls.* Catalysts, 2020. **10**(4): p. 393 DOI: 10.3390/catal10040393
[16] Nasri, Z., *Upgrading vacuum distillation residue of oil refinery using microwave irradiation.* Chemical Engineering and Processing - Process Intensification, 2019. **146**: p. 107675 DOI: https://doi.org/10.1016/j.cep.2019.107675.
[17] Jeon, S.G., et al., *Catalytic pyrolysis of Athabasca bitumen in H2 atmosphere using microwave irradiation.* Chem Eng Res Des, 2012. **90**(9): p. 1292-1296 DOI: 10.1016/j.cherd.2012.01.001.
[18] Li, K., et al., *Application of Carbon Nanocatalysts in Upgrading Heavy Crude Oil Assisted with Microwave Heating.* Nano Lett, 2014. **14**(6): p. 3002-3008 DOI: 10.1021/nl500484d.
[19] Porch, A., et al., *Microwave treatment in oil refining.* Applied Petrochemical Research, 2012. **2**(1): p. 37-44 DOI: 10.1007/s13203-012-0016-4.
[20] Brunauer, S., P.H. Emmett, and E. Teller, *Adsorption of Gases in Multimolecular Layers.* J Am Chem Soc, 1938. **60**(2): p. 309-319 DOI: 10.1021/ja01269a023.
[21] Barrett, E.P., L.G. Joyner, and P.P. Halenda, *The Determination of Pore Volume and Area Distributions in Porous Substances. I. Computations from Nitrogen Isotherms.* J Am Chem Soc, 1951. **73**(1): p. 373-380 DOI: 10.1021/ja01145a126.
[22] Hart, A., et al., *Effect of cyclohexane as hydrogen-donor in ultradispersed catalytic upgrading of heavy oil.* Fuel Process Technol, 2015. **138**: p. 724-733 DOI: https://doi.org/10.1016/j.fuproc.2015.07.016.
[23] Digne, M., *Principles Involved in the Preparation of Hydrotreating Catalysts*, in *Catalysis by transition metal sulphides: From molecular theory to industrial application*, H. Toulhoat and P. Raybaud, Editors. 2013, Editions Technip: Paris, France.
[24] Greensfelder, B.S., H.H. Voge, and G.M. Good, *Catalytic and Thermal Cracking of Pure Hydrocarbons: Mechanisms of Reaction.* Ind Eng Chem, 1949. **41**(11): p. 2573-2584 DOI: 10.1021/ie50479a043.
[25] Hart, A., et al., *Hydrogenation and Dehydrogenation of Tetralin and Naphthalene to Explore Heavy Oil Upgrading Using NiMo/Al2O3 and CoMo/Al2O3 Catalysts Heated with Steel Balls via Induction.* Catalysts, 2020. **10**(5): p. 497 DOI: 10.3390/catal10050497.
[26] Hart, A., et al., *Down-hole heavy crude oil upgrading by CAPRI: Effect of hydrogen and methane gases upon upgrading and coke formation.* Fuel, 2014. **119**: p. 226-235 DOI: https://doi.org/10.1016/j.fuel.2013.11.048.
[27] Richardson, J.F. and D.G. Peacock, *Gas-Solid Reactions and Reactors*, in *Coulson and Richardson's Chemical Engineering Volume 3 - Chemical and Biochemical Reactors and Process Control (3rd Edition)*. 1994, Elsevier.
[28] Fogler, S.H., *Diffusion and Reaction*, in *Elements of chemical reaction engineering*. 2016, Prentice Hall.
[29] Rigby, S.P., *Nuclear Magnetic Resonance and Microscopy Methods*, in *Structural Characterisation of Natural and Industrial Porous Materials: A Manual*. 2020, Springer International Publishing: Cham. p. 89-113.

[30] Bravo-Sanchez, M., et al., *Quantification of the sulfidation extent of Mo in CoMo HDS catalyst through XPS.* Appl Surf Sci, 2019. **493**: p. 587-592 DOI: https://doi.org/10.1016/j.apsusc.2019.07.012.
[31] Liu, Y., et al., *Relating structure and composition with accessibility of a single catalyst particle using correlative 3-dimensional micro-spectroscopy.* Nature Communications, 2016. **7**(1): p. 12634 DOI: 10.1038/ncomms12634.
[32] Zhang, Y.S., et al., *Fine structural changes of fluid catalytic catalysts and characterization of coke formed resulting from heavy oil devolatilization.* Applied Catalysis B: Environmental, 2020. **263**: p. 118329 DOI: https://doi.org/10.1016/j.apcatb.2019.118329.
[33] Rigby, S.P., *Gas Sorption*, in *Structural Characterisation of Natural and Industrial Porous Materials: A Manual*. 2020, Springer International Publishing: Cham. p. 15-48.
[34] Seaton, N.A., *Determination of the connectivity of porous solids from nitrogen sorption measurements.* Chem Eng Sci, 1991. **46**(8): p. 1895-1909 DOI: https://doi.org/10.1016/0009-2509(91)80151-N.
[35] Liu, H., L. Zhang, and N.A. Seaton, *Determination of the connectivity of porous solids from nitrogen sorption measurements — II. Generalisation.* Chem Eng Sci, 1992. **47**(17): p. 4393-4404 DOI: https://doi.org/10.1016/0009-2509(92)85117-T.
[36] Liu, H. and N.A. Seaton, *Determination of the connectivity of porous solids from nitrogen sorption measurements—III. Solids containing large mesopores.* Chem Eng Sci, 1994. **49**(11): p. 1869-1878 DOI: https://doi.org/10.1016/0009-2509(94)80071-5.
[37] Mann, R., *Catalyst deactivation by coke deposition: Approaches based on interactions of coke laydown with pore structure.* Catal Today, 1997. **37**(3): p. 331-349 DOI: https://doi.org/10.1016/S0920-5861(97)00023-0.